Dynamics of cascaded Brillouin–Rayleigh scattering in a distributed fiber Raman amplifier

Kap-Dong Park

Condensed Matter Research Institute, School of Physics, and Optical Communication Systems Laboratory, School of Electrical Engineering and Computer Science, Seoul National University, Seoul 151-742, Korea

Bumki Min, Pilhan Kim, and Namkyoo Park

Optical Communication Systems Laboratory, School of Electrical Engineering and Computer Science, Seoul National University, Seoul 151-744, Korea

Jai-Hyung Lee and Joon-Sung Chang

Condensed Matter Research Institute, School of Physics, Seoul National University, Seoul 151-742, Korea

Received August 29, 2001

We investigate the dynamics of a novel multiwavelength generator in which cascaded–stimulated Brillouin scattering and Rayleigh scattering are automatically balanced to given an evenly spaced (9.4-GHz), highly flattened (<3-dB) optical frequency comb over a 57.2-nm span. The extended effective length for the relevant nonlinear processes from the distributed Raman gain and the reduced Brillouin threshold from the seeding effect of Rayleigh backscattered waves are considered to be the key factors that explain the operation of this structure. © 2002 Optical Society of America

OCIS codes: 290.5870, 290.5900, 290.5910.

Multiwavelength fiber lasers have been a topic of extensive study for past decade, with their application potentials in optical communications, sensors, and terahertz frequency generation.[1–3] Of the various approaches to these applications that use different materials and phenomena, the use of Brillouin fiber lasers (BFLs) has not been considered seriously because of the inefficiency of these lasers for the generation of multiple lines. For example, Fabry–Perot-cavity-based BFLs[4] demonstrated so far do not have more than 14 Brillouin-shifted lines. Even with many complex cavity structures and multiple gain media for the BFLs, the number of lasing lines is still limited to fewer than 55, with consequent undesirable power flatness.[5,6] These limitations in the lasing bandwidth, power, and complex optimization have made the application of multiwavelength lasers difficult.

In this Letter we propose and analyze the dynamics of a novel multiwavelength Brillouin-shifted comb generator, which to our knowledge is a first demonstration of a BFL under Raman gain—a totally distinct, new approach. With the use of stimulated Brillouin scattering in a distributed Raman gain medium, we demonstrate the possibility of >1000-channel, equal-amplitude cascaded Brillouin operation of the comb generator without any kind of reinjection port or ring structure. For this generator, distributed, inhomogeneous Raman gain permits a longer interaction length and excellent stability in the nonlinear processes. The amplified Brillouin–Rayleigh backscattered light in the medium also provides self-feedback–seeding–clamping effects for the efficient generation of amplitude-flattened multi-Stokes lines without the need for complex structures.

The configuration of the multiwavelength comb generator is illustrated in Fig. 1. For the efficient generation of a first Brillouin–Stokes line, we employed a tunable external-cavity laser with a narrow linewidth as a Brillouin pump (BP) source. We used 11.2 km of dispersion-compensating fiber (DCF) with small core size as a highly nonlinear Raman–Brillouin gain medium. Two Raman pumps, from 1465- and 1480-nm laser diode (LDs), were combined with a 1465/1480 coupler (WDM 4) and then injected into the DCF through a 1480/1550 coupler (WDM 3). A high-power ytterbium-doped fiber laser (YFL; 1060 nm, 10 W) was also coupled to the DCF through 1060/1550 couplers (WDM 1 and WDM 2), not only to generate sixth-order Raman Stokes lines at 1471 nm but also to amplify two Raman pump waves from the 1465- and 1480-nm laser diodes. This multiple Raman pumping scheme provides even higher and wider Raman gain over a 1540–1610-nm range. Also included in the setup was a reflecting mirror (connected to WDM 2) to reinject the backscattered lower-order Raman–Stokes line back into the DCF for enhancement of the Raman gain efficiency.

To verify the effect of distributed Raman gain on Brillouin–Rayleigh scattering we first measured forward and backward Brillouin–Rayleigh spectra with the 1465-nm Raman pump only. Figure 2(a) shows the effect of distributed Raman gain on the

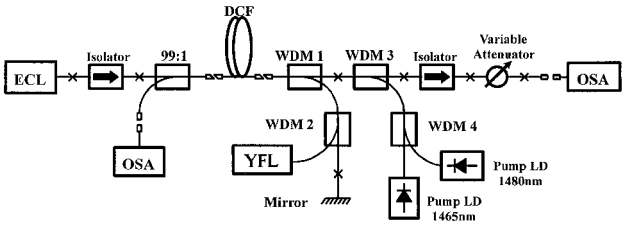

Fig. 1. Experimental setup: abbreviations are defined in text.

0146-9592/02/030155-03$15.00/0

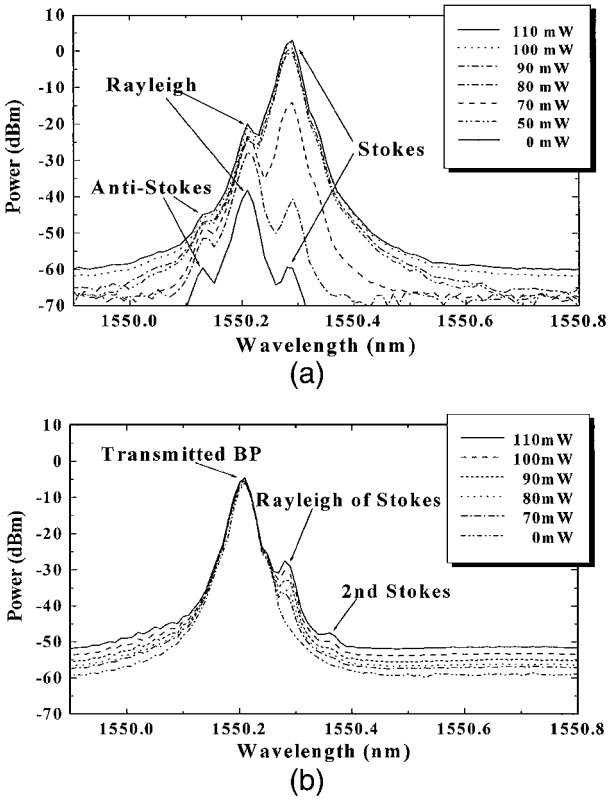

Fig. 2. Effects of Raman pump power on (a) backward-propagating spectral lines and (b) forward-propagating spectral lines (resolution bandwidth, 0.01 nm with the 1465-nm pump on and the 1480-nm YFL power off).

powers of backward-propagating light [measured at the optical spectrum analyzer (OSA) 1 in Fig. 1] in our configuration curves of the increasing powers of the 1465-nm Raman pump are defined in the inset. The lowest trace in Fig. 2(a) corresponds to 1550.21-nm BP input and no Raman pump injection. Rayleigh backscattered light (frequency unshifted) and Brillouin–Stokes (frequency redshifted, +0.078 nm) and anti-Stokes (frequency blueshifted, −0.078 nm) lines were observed as a result of spontaneous scattering in the DCF.[7] At first, the Rayleigh component showed much higher power than the other two lines without the Raman gain, as a result of the high Landau–Placzek ratio (estimated to be 40 in a DCF and 30 in a single-mode fiber).[8]

In contrast, with increasing Raman pump injection into the fiber the Brillouin-Stokes line grew much faster and saturated to a constant level owing to its low nonlinear threshold power,[9] whereas the other two lines exhibited below-threshold behavior with linear dependence on the pump power.

After saturation, the first Brillouin–Stokes line initiated the onset of the second Brillouin–Stokes line in the forward direction, inducing a subsequent power transfer to higher orders [Fig. 2(b); measured at the right most optical spectrum analyzer in Fig. 1). The observed Landau–Placzek ratio and the characteristics of the spectral growth relative to Raman pump power were similar to those for a backward spectrum.

To further see the effect of Raman gain on successive Stokes line generation, we turned on a 1480-nm Raman pump and a YFL in addition to the 1465-nm Raman pump to provide even higher Raman gain over a 1540–1610-nm range. Figure 3 shows a closer view of forward and backward spectra overlaid in the same figure, with the YFL power near threshold for generation of a second Brillouin–Stokes line. There was a critical power of YFL near 4.8 W, above which all the Stokes lines appeared quasi simultaneously (for both directions) over the entire Raman gain range. In this figure the zeroth-order line at 1547.08 nm is the wavelength of the transmitted BP in the forward direction. In the forward spectrum the even-order lines (except at zeroth order) correspond to higher-order Brillouin–Stokes lines, and the odd-order lines are Rayleigh components that have been backscattered by a Brillouin–Stokes line propagating in reverse direction. Because the threshold power of Rayleigh scattering is higher than that of Brillouin scattering in a DCF, the power difference between the two lines is attributed to the conditions for above-threshold–below-threshold Brillouin–Rayleigh scattering. In addition to the power difference, one can observed a difference in 3-dB bandwidth between even- and odd-order lines. Recall the differences in the origin of these waves: the odd channel (in the forward direction) is the amplified Rayleigh backscattered wave from a Brillouin–Stokes line and the even channel is the Brillouin–Stokes wave from a backward-propagating Brillouin–Stokes line. Thus the bandwidth dissimilarity can be easily understood: In general, the bandwidth of Brillouin scattering is broader than that of Rayleigh scattering.[10] For the backward spectrum (dashed curve in Fig. 3) the odd-order lines correspond to Brillouin–Stokes lines and the even orders Rayleigh components of a forward-propagating higher Stokes line. The difference in amplitude for Rayleigh components in the forward and backward directions is attributed to the dependence of Raman gain efficiency on pumping direction in our experimental setup.[11] Except for the first few channels, higher-order channels show extremely flat spectra because of the inhomogeneous, flat Raman gain profile. For this operation the first

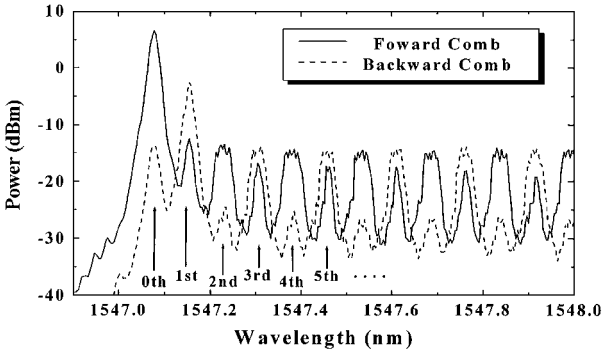

Fig. 3. Comb profile near the critical pump power (forward–backward spectrum. Resolution bandwidth, 0.01 nm with all the three pumping sources on).

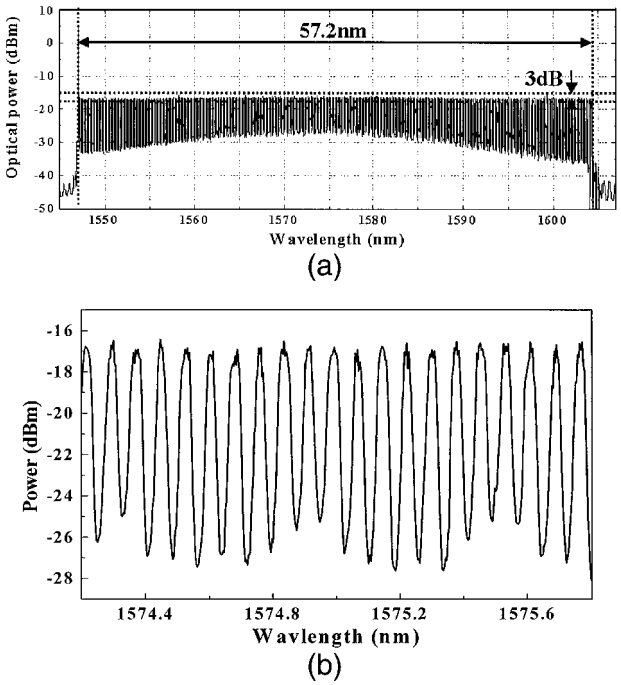

Fig. 4. Closer look at (a) the optimized multiwavelength comb over (b) the full spectral range near the center. Resolution bandwidth 0.01 nm.

Brillouin–Stokes line amplified by Raman gain grows to reach a second Brillouin–Stokes threshold, which acts as a new Brillouin input pump for subsequent Brillouin–Stokes generation. Rayleigh components that are concurrent with Brillouin–Stokes components grow as well with Raman gain, and their coupled presence in this process reduces the threshold power for subsequent Brillouin–Stokes beams.[12]

When the YFL output was further increased above the critical power for comb generation (4.8 W), the output powers of the Brillouin components remained at a constant level owing to the threshold behavior of stimulated Brillouin scattering, and the subsequent transfer of power to neighboring higher-order Stokes lines. In contrast, the powers of Rayleigh components increased linearly, finally reaching the same power level as the Brillouin–Stokes components. We then finally adjusted the flatness and the number of comb lines by changing the power of the YFL, the 1465–1480-nm Raman pumps, and the Brillouin pump wavelength.

Figure 4 shows one of the optimization results, for best flatness, with a YFL power of 6.2 W and a 4-dBm Brillouin pump at 1547.08 nm. Figure 4(a) shows the forward-propagating Brillouin comb cascade over 57.2 nm, over the entire spectral range. The saturated output power of each line was ~ -17 dBm, with power deviation of less than 3 dB. A closer view of the spectrum, measured with an optical spectrum analyzer (resolution bandwidth, 0.01 nm), is shown in Fig. 4(b). For this operation regime there was no spectral difference between Brillouin components and Rayleigh components. As the Brillouin pump input wavelength shifted toward the center of the multiwavelength comb spectrum, the saturation power of each line increased a little, but the number of comb lines decreased linearly while the total output power of all the lines remained the same. When the YFL power was increased far above threshold, a seventh-order Raman Stokes line at 1575 nm became dominant above the Stokes channel power and terminated the generation of the Brillouin-shifted multiwavelength comb.

In conclusion, we have proposed, demonstrated, and identified the self-feedback mechanism of Brillouin–Rayleigh backscattering in the presence of distributed Raman gain. Because of fast power growth and the increased interaction length that results from distributed Raman gain, the Brillouin-scattered light works as a new Brillouin pump source for subsequent Stokes line generation in the reverse direction. Brillouin-shifted combs over a span of 57.2 nm with high degrees of flatness and stability were obtained through simple optimization of a Raman gain profile and Brillouin pump power and wavelength. By investigating the difference in peak power between the odd- and the even-order Stokes lines under insufficient Raman gain, we also identified the role of amplified Rayleigh scattering in this configuration. The flexible power scalability and wavelength selectivity of Raman amplifiers promise that this approach will be a unique means of generating multiwavelength combs over even wider spectral ranges. It also should be possible to adapt various schemes for multiwavelength generation by utilizing this operational principle.

K.-D. Park's e-mail address is kdpark@stargate.snu.ac.kr.

References

1. J. Chow, IEEE Photon. Technol. Lett. **8,** 60 (1996).
2. N. Park, IEEE Photon. Technol. Lett. **8,** 1459 (1996).
3. S. Yamashita and K. Hotate, Electron. Lett. **32,** 1298 (1996).
4. K. O. Hill, D. C. Johnson, and B. S. Kawasaki, Appl. Phys. Lett. **29,** 185 (1976).
5. G. J. Cowle, in *Optical Fiber Communication Conference*, Vol. 6 of 1997 OSA Technical Digest Series (Optical Society of America, Washington, D.C., 1997), pp. 34–35.
6. K.-D. Park, in *Optical Fiber Communication Conference*, 2000 OSA Technical Digest Series (Optical Society of America, Washington, D.C., 2000), pp. 11–13.
7. I. L. Fabelinskii, *Molecular Scattering of Light* (Plenum, New York, 1968).
8. G. P. Lees, P. C. Wait, M. J. Cole, and T. P. Newson, IEEE Photon. Technol. Lett. **10,** 126 (1998).
9. G. P. Agrawal, *Nonlinear Fiber Optics*, 2nd ed. (Academic, San Diego, Calif., 1995).
10. W. Kaiser and M. Maier, *Laser Handbook* (North-Holland, Amsterdam, 1972), Vol. 2.
11. K. Mochizuki, J. Lightwave Technol. **LT-4,** 1328 (1986).
12. K. Inoue, Opt. Commun. **120,** 34 (1995).